



CHORUS

This is the accepted manuscript made available via CHORUS. The article has been published as:

4π Josephson currents in junctions of hybridized multiband superconductors

T. O. Puel, P. D. Sacramento, and M. A. Continentino

Phys. Rev. B **95**, 094509 — Published 15 March 2017

DOI: [10.1103/PhysRevB.95.094509](https://doi.org/10.1103/PhysRevB.95.094509)

4 π -Josephson currents in junctions of hybridized multiband superconductors

T.O. Puel^{1,*}, P.D. Sacramento^{1,2}, and M. A. Continentino¹

¹*Centro Brasileiro de Pesquisas Físicas, Rua Dr. Xavier Sigaud, 150, Urca 22290-180, Rio de Janeiro, RJ, Brazil and*

²*CeFEMA, Instituto Superior Técnico, Universidade de Lisboa, Av. Rovisco Pais, 1049-001 Lisboa, Portugal*

(Dated: January 31, 2017)

We study two-band one-dimensional superconducting chains of spinless fermions with inter and intra-band pairing. These bands hybridize and, depending on the relative angular momentum of their orbitals, the hybridization can be symmetric or anti-symmetric. The self-consistent competition between intra and inter-band superconductivity and how it is affected by the symmetry of the hybridization is investigated. In the case of anti-symmetric hybridization the intra and inter-band pairings do not coexist while in the symmetric case they do coexist and the interband pairing is shown to be dominant. The topological properties of the model are obtained through the topological invariant winding number and the presence of edge states. We find the existence of a topological phase due to the inter-band superconductivity and induced by symmetric hybridization. In this case we find a characteristic 4 π -periodic Josephson current. In the case of anti-symmetric hybridization we also find a 4 π -periodic Josephson current in the gapless inter-band superconducting phase, recently identified to be of Weyl-type.

PACS numbers: 74.50.+r, 74.20.-z, 03.65.Vf

I. INTRODUCTION

Traditional models of topological superconductors only consider a single band even though this is usually a simplification. At the single-band level it is well known that the single-band Kitaev model¹⁻³ – anti-symmetric pairs of spinless fermions in 1D with an effective spin triplet pairing – is the simplest model that exhibits a topological phase with Majorana modes in the ends of a p -wave chain, depending on the state of the system. In the trivial phase, the chain is superconducting with no end states³. Triplet superconductivity is, however, rare in nature. Thus, the pursuit of alternatives to create triplet superconductivity lead to engineering a topological insulating chain (made with strong spin-orbit material) in proximity of a normal superconductor and in the presence of an applied magnetic field⁴⁻⁹. Another proposal for an effective one-dimensional model considered placing magnetic impurities on top of a conventional or triplet superconductor¹⁰⁻¹² increased the interest on the realization of an effective one-dimensional system with topological properties¹³⁻¹⁵. Additionally, triplet pairing has been found to be physically realizable in some systems. In Ref. [16] it was shown that odd-parity superconductivity occurs in superconducting (SC) multilayers, where this state is a symmetry-protected topological state. In addition, triplet pairing is found in ³He¹⁷ and in Sr₂RuO₄¹⁸, as well as in some rare noncentrosymmetric systems¹⁹. Triplet pairing was also studied in the context of extended Hubbard chain²⁰.

Multiband models for the superconducting state and their topological properties have also received increasing attention recently^{16,21-25}. This consideration has been important to explain many important effects in topological systems. For instance, topological semimetals²⁶ and chiral superfluidity²⁷ have been predicted in multiorbital

models where orbitals with different symmetries interact. Two component fermionic systems with occupied s and p orbital states were shown to have a rich phase diagram in both one and two dimensions²⁴. A general connection between multiband and multicomponent superconductivity has also been made²⁸. Topological properties in three-band models were also studied²⁹⁻³². The interest in multiband bands is also justified for instance in studies of three-dimensional $Cu_xBi_2Se_3$ which has two orbitals per lattice cell. This leads in general to multipocket Fermi surfaces that in the case of odd number may be topological³³⁻³⁵. Another proposed example of a multiband superconductor with triplet $p + ip$ pairing is Sr_2RuO_4 , referred above.

An interesting example of a multiband system with non-trivial edge states are the zigzag edges of monolayer transition metal-dichalcogenides for which it has been proposed that under appropriate conditions, such as due to the presence of intrinsic spin-orbit coupling, proximity coupled to a conventional superconductor and an in-plane magnetic field, the edges display Majorana edge states³⁶⁻³⁸. Under these conditions the system is equivalent to the Kitaev chain that in the simplest case reduces to only one band in the vicinity of the chemical potential. More complex situations may be explored that involve the presence of more bands (a minimal model considers three orbitals). A strictly one-dimensional multiband model that has a topological nature is the SSH model for polyacetylene³⁹ that, when coupled to a triplet superconductor (such as for instance Sr_2RuO_4), leads to an interesting problem of a dimerized superconductor (two bands) with different types of edge states. In one regime is equivalent to the Kitaev model (with one edge mode at each edge) and in another regime displays two edge modes (winding number two)⁴⁰, which are however of a fermionic type and not of Majorana

type. Other possible realizations of the model are engineering the Rashba spin-orbit interaction by placing micromagnets^{41–47} or quantum-dot array⁴⁸. The realistic presence of longer range hoppings or pairings in a Kitaev like model leads to a multiplicity of edge Majorana modes and complex phase diagrams^{49–52}. In general this problem is equivalent to a multiband system. Experimentally this can be achieved considering two or more magnetic chains superimposed on a two-dimensional conventional superconductor^{11,53}. For instance, considering two chains this is equivalent to a two band model.

Motivated by the recently discussed topological characters of multiband models^{16,24}, and based on the simplest model that describes the topological properties of a chain of spinless fermions, we study the Kitaev model with two orbital-bands. We include and discuss inter- and intra-band superconducting couplings. A characteristic feature of multiband systems is the hybridization between the different orbitals. This arises from the superposition of the wave functions of these orbitals in different sites. It can have distinct symmetry properties depending on the orbitals involved. If this mixing involves orbitals with angular momenta that differ by an odd number, hybridization turns out to be anti-symmetric, i.e., in real space we have $V_{ij} = -V_{ji}$ or in momentum, k -space, $V(-k) = -V(k)$. Otherwise hybridization is symmetric respecting inversion symmetry in different sites⁵⁴.

The bulk-edge correspondence guarantees that in the topological phases there are subgap edge states. In the case of a topological superconductor, zero energy Majorana modes are predicted to appear and great effort has been devoted to prove their existence. Methods that provide signatures of their presence have been proposed and experimentally tested via for instance tunneling experiments^{55,56}, interferometry³, point contacts using the Andreev reflection⁵⁷ through the detection of zero-bias peaks⁵⁸, using the quantum waveguide theory⁵⁹ which gives the correct bulk-edge correspondence³⁵ and fractional Josephson currents^{1,3,60}. Also signatures of the Majorana states may be found in bulk measurements such as the imaginary part of frequency dependent Hall conductance⁶¹ and the d.c. Hall conductivity itself⁶².

The existence of topological phases is detected in this work numerically calculating the winding number and by showing the existence of edge states at the ends of the chain. In addition, we calculate the Josephson current across the junction between two superconductors to identify regimes where the periodicity of the Josephson current on the phase differences between the superconductors (original proposal by Kitaev¹) or the equivalent situation of a superconducting ring threaded by a magnetic flux and interrupted by an insulator changes from the usual value of 2π to a 4π value⁶³. As shown before^{1,63–73} the existence of the Majoranas at the edges allows tunneling of a single fermion at zero-bias leading to a 4π -periodic current in contrast to the usual Cooper pair transport across the junction which leads to the usual 2π -periodic current. Experimental realization to

detect 4π -periodic Josephson junction has been presented in Ref. [74] and an application to multiband systems has recently been presented in Ref. [75].

II. MODEL AND SELF-CONSISTENT CALCULATIONS

We consider a two-band superconductor with hybridization and triplet pairing in 1D, i.e., a chain of sites supporting two orbitals, let's say orbitals A and B . The pairing between fermions may exist on different bands (inter-band) or in each band (intra-band) and are always of p -wave type, in the sense that pairs of spinless fermions are spatially anti-symmetric. The problem can be viewed as a generalization of the Kitaev model to two orbitals. We also have the hybridization term between the orbitals A and B that may be symmetric or anti-symmetric. The simplest Hamiltonian in momentum space that describes those types of superconductivity and hybridization may be written as $\mathcal{H} = \mathcal{H}_0 + \mathcal{H}_h + \mathcal{H}_{SC}$ where the kinetic part is

$$\mathcal{H}_0 = \sum_k \left\{ (\varepsilon_k^A - \bar{\mu}) a_k^\dagger a_k + (\varepsilon_k^B - \bar{\mu}) b_k^\dagger b_k \right\}, \quad (1)$$

where a_k^\dagger (b_k^\dagger) is the creation operator of spinless fermion at A (B)-band with momentum k . Also, $\bar{\mu}$ is the chemical potential and $\varepsilon_k^A, \varepsilon_k^B$ are the band hopping energies. The hybridization term is

$$\mathcal{H}_h = \sum_k \left\{ V(k) a_k^\dagger b_k - V(-k) b_{-k} a_{-k}^\dagger + \text{h.c.} \right\}, \quad (2)$$

where $V(k) = 2iV_{as} \sin(k) \equiv V_{as,k}$ if the hybridization is anti-symmetric or $V(k) = 2V_s \cos(k) \equiv V_{s,k}$ if the hybridization is symmetric, and V is the hybridization amplitude. Finally, the mean-field superconducting contribution to the Hamiltonian is

$$\mathcal{H}_{SC} = \sum_k \left\{ \Delta_k a_k^\dagger b_{-k}^\dagger + \Delta_k b_k^\dagger a_{-k}^\dagger + \Delta_{A,k} a_k^\dagger a_{-k}^\dagger + \Delta_{B,k} b_k^\dagger b_{-k}^\dagger + \text{h.c.} \right\}, \quad (3)$$

with $\Delta_k = i\Delta \sin(k)$ where Δ is the superconducting inter-band pairing amplitude, and $\Delta_{(A,B),k} = i\Delta_{(A,B)} \sin(k)$ where Δ_A and Δ_B are the superconducting intra-band pairing amplitudes. We could also include a superconducting term that changes Cooper pairs between different orbitals, which in terms of two particles interaction may be written as $\sum_{k,k'} g_J(k,k') (b_k^\dagger b_{-k}^\dagger a_{-k'} a_{k'} + a_k^\dagger a_{-k}^\dagger b_{-k'} b_{k'})$, where g_J is the interaction strength. Without fluctuation, i.e., in the BCS theory, this term appears as an additive parameter to Δ_A and Δ_B , thus besides enhancing the intra-band superconductivity it does not change qualitatively the topological properties of the Hamiltonian considered here.

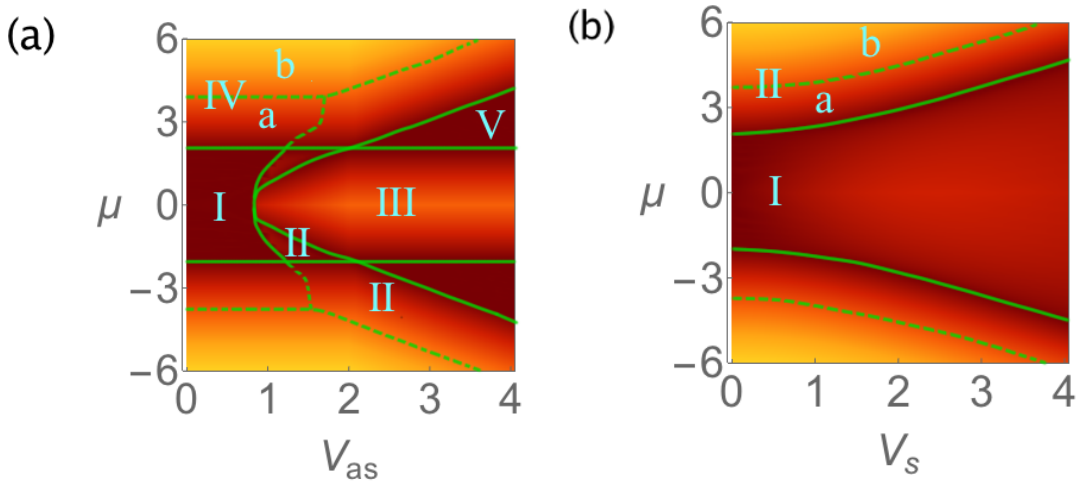


Figure 1. The left panel shows the phase diagram for anti-symmetric hybridization, for different values of chemical potential μ and hybridization V_{as} , both normalized by the hopping amplitude t . Phase I is a gapless inter-band superconducting phase. II is a gapped intra-band superconducting phase. III is a topological insulating phase. IVa shows a trivial gapped inter-band SC. IVb is a trivial insulating phase. Finally, V is a metallic phase. The phase diagram for the symmetric case is shown on the right panel. Phase I carries both types of pairings and has non-trivial topological properties. Phase IIa is a gapped superconducting phase also with both inter- and intra-band pairings, but trivial topological properties. Phase IIb is a normal insulator. Both phase diagrams are symmetric around $\mu = 0$ and we show the results for $g/2 = g_A = g_B = 1.7$. The solid lines represent a gap closing, while the dashed lines represent a phase separation without closing the gap.

In the more compact BdG form, the Hamiltonian may be written in the Nambu representation⁷⁶ as $\mathcal{H} = \sum_k \mathbf{C}_k^\dagger \mathcal{H}_k \mathbf{C}_k$, where $\mathbf{C}_k^\dagger = (a_k^\dagger b_k^\dagger a_{-k} b_{-k})$ and

$$\begin{aligned} \mathcal{H}_k = & -\mu \Gamma_{z0} - \varepsilon_k \Gamma_{zz} + \Delta_k i \Gamma_{yx} \\ & + \Delta_{A,k} \frac{1}{2} (i \Gamma_{y0} + i \Gamma_{yz}) + \Delta_{B,k} \frac{1}{2} (i \Gamma_{y0} - i \Gamma_{yz}) \\ & + V_k \cdot \mathbb{I}, \end{aligned} \quad (4)$$

where $\Gamma_{ij} = \tau_i \otimes s_j$, $\forall i, j = 0, x, y, z$; τ and s are the Pauli matrices acting on particle-hole and sub-band spaces, respectively, and $s_0 = \tau_0$ are the 2×2 identity matrices. Also, for convenience, we have defined $-\mu = (1/2)(\varepsilon_k^A + \varepsilon_k^B) - \bar{\mu}$ as the chemical potential relative to the hopping energies of the bands and the hopping energy $(1/2)(\varepsilon_k^A - \varepsilon_k^B) = 2t \cos(k) \equiv \varepsilon_k$ as the difference between the bands energies, where t is the hopping amplitude. With respect to the Hamiltonian parameters: $V_k = V_{as,k} i \Gamma_{zy}$ if the hybridization is anti-symmetric or $V_k = V_{s,k} \Gamma_{zx}$ if the hybridization is symmetric.

The Hamiltonian defined in Eq. (4) can be solved using BdG transformations. The self-consistent solution implies that the pairings can be obtained using

$$\Delta = g \frac{1}{L} \sum_k i \sin(k) (\langle a_k b_{-k} \rangle + \langle b_k a_{-k} \rangle), \quad (5)$$

$$\Delta_A = g_A \frac{2}{L} \sum_k i \sin(k) \langle a_k a_{-k} \rangle, \quad (6)$$

$$\Delta_B = g_B \frac{2}{L} \sum_k i \sin(k) \langle b_k b_{-k} \rangle, \quad (7)$$

where g , g_A and g_B are the strength of the interactions

between fermions in different orbitals, in orbitals A and in orbitals B , respectively.

A. Phase diagrams

In Fig. 1 we show the phase diagrams for the symmetric and anti-symmetric hybridization. The latter is included for comparison since a very similar diagram was reported in ref. [77]. The solid lines represent a gap closing, while the dashed lines represent a phase separation without closing the gap. As we can see, the consideration of inter-band, intra-band superconductivity and (anti-)symmetric hybridization results in rich phase diagrams.

In the left panel, for anti-symmetric hybridization, phase I is a gapless superconducting phase, driven by the inter-band coupling, and it was shown⁷⁷ to behave like Weyl superconductor. The phase II is a two-band superconductor with only intra-band couplings. Phase III is a topological insulator. The phase IVa shows gapped superconductivity and represents the strong inter-band coupling superconducting phase. The phase IVb is a trivial insulator. Finally, phase V is a normal metallic phase. All those phases are symmetric around $\mu = 0$. Since the intra- and inter-band pairings do not coexist, the phases with no intra-band pairing are similar to the results previously obtained⁷⁷. The main difference results from the appearance of the intra-band pairing in some regions of the phase diagram.

The right panel is for the symmetric case. Phase I and IIa are gapped superconducting phases, with the co-

existence of inter- and intra-band couplings, but dominated by the inter-band one. Phase IIb is an insulating phase and there is no SC. All those phases are symmetric around $\mu = 0$. The more interesting phase is phase I, which allows both types of couplings and shows non-trivial topological properties. This phase is characterized by localized edge states and finite winding number, as will be shown in the next section.

Consider the case of symmetric hybridization (V_s), when the orbitals angular momenta have equal parities, like orbitals s and d . In Figs. 1 we show the results for $g/2 = g_A = g_B = 1.7$. First, we notice that the intra-band SC distinguishes between different bands, since there is a change of sign between them. Unlike the anti-symmetric case, here there is a coexistence of inter- and intra-band SC. Remarkably, the inter-band has the larger order parameter for all region of parameters. In general, this indicates that the inter-band SC has higher critical temperature, which turns out to be responsible for the superconductivity appearing in the material. Note that symmetric hybridization is responsible for the emergence of intra-band SC. Very strong symmetric hybridization eventually destroys superconductivity.

The strength of the coupling g itself only changes the superconducting amplitude of the SC phases (inter- or intra-band ones), thus its choice does not change qualitatively the results presented. It is interesting to point out that the self-consistent results for the superconducting order parameters may converge to different results depending on the initial guesses. This is a consequence of the first order nature of the quantum phase transitions between the different ground states. Therefore it is necessary to calculate the energy of the different states to obtain the true ground state for a given set of parameters.

III. TOPOLOGICAL PROPERTIES

A. Winding number in the BDI class

The Hamiltonian of equation (4) has particle-hole symmetry and simplified time reversal symmetry for spinless fermions⁷⁸. In the presence of both symmetries, the Hamiltonian belongs to the BDI class of topological systems, and the one-dimensionality guarantees that the space of the quantum ground state is partitioned into topological sectors labeled by an integer (\mathbb{Z}) number^{78,79}.

Proceeding with the standard calculation the winding number^{79,80}, the Chiral operator Γ_{x0} brings the Hamiltonian to the block off-diagonal form

$$R^{-1} \mathcal{H}_k R = \begin{pmatrix} 0 & q(k) \\ q^\dagger(k) & 0 \end{pmatrix}, \quad (8)$$

where $R = \Gamma_{xx} - \Gamma_{zx}$. Writing a generic Hamiltonian in the form

$$\mathcal{H}_k = \sum_{i,j} h_{ij} \Gamma_{ij}, \quad i, j = 0, x, y, z, \quad (9)$$

whose coefficients h_{ij} may be extracted from any generic Hamiltonian \mathcal{H} through $h_{ij} = \frac{1}{4} \text{Tr}(\Gamma_{ij} \mathcal{H})$, if we apply the PHS to Eq. (9) as $\mathcal{H}_k = -\Gamma_{x0} \mathcal{H}_{-k}^T \Gamma_{x0}$ and proceed with the block off-diagonal calculations described above we find that

$$q(k) = \sum_j c_j (h_{zj} + i h_{yj}) \sigma_j, \quad j = 0, x, y, z, \quad (10)$$

where $c_0 = c_x = +1$ and $c_y = c_z = -1$, $\sigma_{x,y,z}$ are the Pauli matrices and σ_0 is the 2×2 identity matrix.

The winding number, W , is defined as the number of revolutions of $\det[q(k)] = m_1(k) + i m_2(k)$ around the origin in the complex plane when k changes from $-\pi$ to π ,

$$W = \frac{1}{2\pi} \int_{-\pi}^{\pi} \frac{\partial \theta(k)}{\partial k} dk, \quad (11)$$

with

$$\theta(k) = \arg \det[q(k)] = \tan^{-1} \frac{m_2(k)}{m_1(k)}. \quad (12)$$

For the generic case considered above we have that

$$\begin{aligned} m_1(k) &= \sum_j d_j (h_{zj}^2 - h_{yj}^2) \\ &\text{and} \\ m_2(k) &= -i \sum_j d_j (2h_{zj} h_{yj}), \end{aligned} \quad (13)$$

where $d_0 = +1$ and $d_{x,y,z} = -1$.

Results – The topological numbers calculations to the anti-symmetric case are discussed in ref. [77]. If we compare Eq. (4) – with symmetric hybridization $V_{s,k}$ – and Eqs. (13) we have $m_1(k) = \mu^2 - \Delta_k^2 - \Delta_{0,k}^2 - V_{s,k}^2 - \epsilon_k^2$ and $m_2(k) = -2(V_{s,k} \Delta_k + \epsilon_k \Delta_{0,k})$. We have considered the case of $\Delta_B = -\Delta_A = \Delta_0$ which came from the self-consistent results. This suggests that the symmetric hybridization may induce a topological phase, since we have non-vanishing m_2 even zero chemical potential. To be sure that the phase is topological we must calculate the winding number itself, or see if the parametric plot of $\bar{m}_1(k)$ and $\bar{m}_2(k)$ contains the origin when $k \in [-\pi, \pi]$. The results for the winding number and the parametric plot are shown in Fig. 2 for the parameters $V_s = 1.2$, $\mu = -1.04$. This figure shows that the parametric plot wraps the origin twice; it means that the winding number in this case is two, $W = 2$. The results for the winding number clearly show the topological phase, induced by symmetric hybridization, and dominated by inter-band superconductivity for small values of the chemical potential that grows as the hybridization, V_s , grows.

B. Edge states in a finite chain

In order to find the energy spectrum of a finite chain of fermions through the BdG transformation we write the

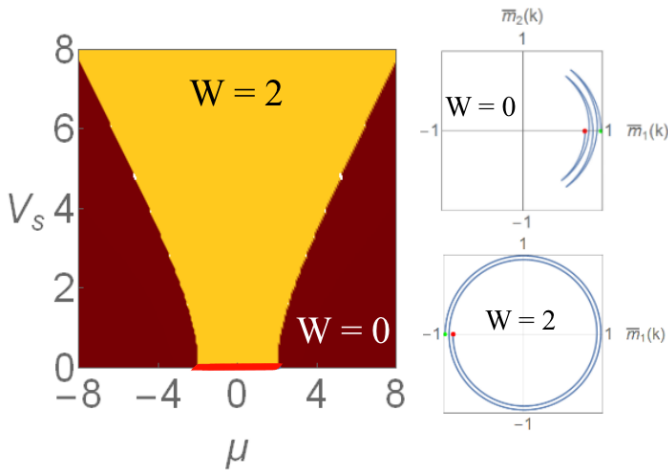


Figure 2. In the left panel we show the winding number calculated from the self-consistent results for symmetric hybridization, over the phase space of parameters. The red line in $V_s = 0$ highlight the fact that the system is gapless in that region and $W = 0$. In the right panels we show the normalized parametric plot of real and imaginary parts of $\det[q(k)]$. The number of times $\det[q(k)]$ wraps the origin is the winding number and is illustrated in the right side.

Hamiltonian, Eq. (4) transformed to real space, in the form

$$\mathcal{H} = \mathbf{C}^\dagger \mathbf{H} \mathbf{C}, \quad (14)$$

where

$$\mathbf{C} = (a_1 \ b_1 \ a_1^\dagger \ b_1^\dagger \ \cdots \ a_N \ b_N \ a_N^\dagger \ b_N^\dagger)^T \quad (15)$$

and the operators a_i^\dagger (a_i) and b_i^\dagger (b_i) create (annihilate) a fermion in the orbital A and B, respectively, at position i in the chain. The matrix \mathbf{H} is defined as

$$\mathbf{H} = \begin{pmatrix} \mathcal{H}_{11} & \cdots & \mathcal{H}_{1N} \\ \vdots & \ddots & \vdots \\ \mathcal{H}_{N1} & \cdots & \mathcal{H}_{NN} \end{pmatrix}, \quad (16)$$

and is comprised by the following (4×4) interaction matrices

$$\begin{cases} \mathcal{H}_{r,r} &= -\mu \Gamma_{z0}, \\ \mathcal{H}_{r,r+1} &= -t \Gamma_{zz} - i \frac{\Delta}{2} \Gamma_{yx} - i \frac{\Delta_0}{2} \Gamma_{y0} + V(r+1), \\ \mathcal{H}_{r,r-1} &= -t \Gamma_{zz} + i \frac{\Delta}{2} \Gamma_{yx} + i \frac{\Delta_0}{2} \Gamma_{y0} + V(r-1), \\ \mathcal{H}_{r,r'} &= 0 \quad \forall r' \neq r, r+1 \text{ or } r-1, \end{cases} \quad (17)$$

where $V(r+1) = -V(r-1) = -i \frac{V}{2} \Gamma_{zy}$ for anti-symmetric hybridization, and $V(r+1) = V(r-1) = \frac{V}{2} \Gamma_{zx}$ for symmetric one.

Results – Since we have defined the topological region of the parameters, we may analyse the zero-energy modes explicitly through the energy spectrum of a finite chain. Similar results are shown in ref. [77], then we focus here

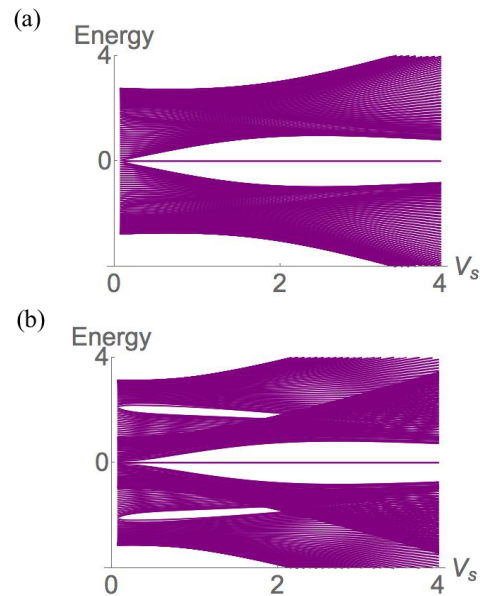


Figure 3. Here we show the energy spectrum of the self-consistent results, for two fixed values of the chemical potential and increasing symmetric hybridization ($\mu = 0$ on (a) and $\mu = -1.4$ on (b)).

on symmetric hybridization. We have calculated the energy spectrum for a chain of $L = 100$ sites, therefore, we get $4L$ energies for the spectrum. We have checked that this size is large enough to prevent finite size effects. We analyze the energy spectrum for two fixed values of chemical potential, $\mu = 0$ and $\mu = -1.4$, and increasing the hybridization according to the self-consistent solution of Fig. 1b. The results are shown in Fig. 3. What we immediately see is that the zero-energy states are robust, i.e., even when μ is non-zero they are present, which characterizes the zero-energy modes in the superconducting phase. We notice that those states are four-fold degenerated. We have checked that they have wavefunctions that are localized exponentially close to the edges if the system is large enough.

IV. 4π JOSEPHSON EFFECT

In the last part of previous section we have considered an open chain, i.e., there was no connection between sites 1 and N . In terms of eq. (17) we have $\mathcal{H}_{N,1} = \mathcal{H}_{1,N} = 0$. Now we may think of a chain as a ring with a Josephson junction coupling the ends, see Fig. 4. An extra hopping term t' couples the end point of the ring to the first point via some insulating junction. If a uniform magnetic field (Φ) flows through this ring, its effect may be captured by a Peierls substitution in the extra hopping term, t'^{81} . Thus, the Josephson junction may be represented by the

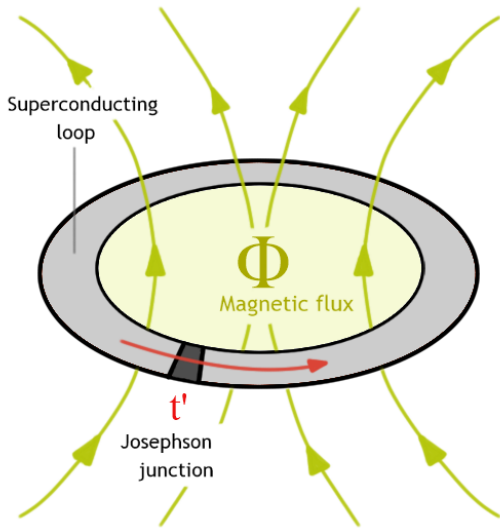


Figure 4. Schematic figure illustrating the 1D superconducting ring with a Josephson junction.

following boundary conditions

$$\mathcal{H}_{N,1} = \mathcal{H}_{1,N}^* = \begin{pmatrix} -e^{-i\phi/2t'} & 0 & 0 & 0 \\ 0 & e^{-i\phi/2t'} & 0 & 0 \\ 0 & 0 & e^{i\phi/2t'} & 0 \\ 0 & 0 & 0 & -e^{i\phi/2t'} \end{pmatrix}, \quad (18)$$

where the superconducting phase difference ϕ across the junction is related to the magnetic flux through the ring by $\phi = 2\pi\Phi/\Phi_0$, and $\Phi_0 = h/2e$ is the superconducting flux quantum. Notice that t' is a tunneling amplitude inversely proportional to a barrier amplitude, across the junction. As mentioned above this is equivalent to the original proposal of the Josephson junction between two different superconductors with different pairing phases also separated by some tunneling amplitude across an insulator (or metal).

Results – we will analyse the topological properties of the system via Josephson junction scheme (Fig. 4). We start looking to the excitation spectrum (bogoliubons) during two pumps for each superconducting phase in the phase diagram.

The anti-symmetric case has three types of superconducting phases: intraband gapped SC, interband gapped SC and interband gapless SC, as shown in Fig. 1a. Both gapped superconducting phases (II and IVa) show similar excitation spectra and their typical bogoliubons that preserves the ground state parity are shown in Fig. 5a. As expected, there are no level crossings in the excitation spectrum and the current is 2π periodic as we can see in Fig. 5a for the case of region IVa. In phase I, even though we have no gap in the bulk spectrum of an infinite system, it is still possible to calculate the Josephson current in a finite one. The junction itself opens up a small gap in the spectrum if L is not too large and t' is not too strong. Of course, in the limit $L \rightarrow \infty$ the gap closes, but

if the tunneling t' is too large (or the barrier too small) the junction just couples both ends analogously to a periodic boundary condition (i.e., infinite system). Thus, a typical excitation spectrum for very small energies in the gap generated by the coupling across the junction (positive and negative excitation) is shown in Figs. 5b and 5c.

Even though Figs. 5b and 5c show no level crossings during the pumps, we may proceed with the derivative of the ground state energy respective to the flux ϕ and obtain the Josephson current. The results are shown in Figs. 5e and 5f for two values of the chemical potential. Clearly, both figures exhibit 4π periodic Josephson current, even without zero energy level crossings revealing in some sense the hidden topological nature of this Weyl-phase.

The results for the symmetric case are shown in Fig. 6, where the first row shows the fig. 6a for the trivial phase IIa, whereas figs. 6b and 6c are for the topological phase I for two values of the chemical potential. Second row of Fig. 6 shows the current flowing through the junction. We clearly see that the current has a periodicity of 2π (one pump) in the trivial phase, Fig. 6d. On the other hand, the periodicity of the Josephson currents in Figs. 6e and 6f are 4π (two pumps), characterizing the topological superconducting phase and providing an alternative evidence for the presence of Majorana states.

V. CONCLUSIONS

In this paper we have studied a model of a p -wave, one dimensional, multiband superconductor. This represents a generalization of the single band model for odd-parity superconductivity that gives rise to a much richer phase diagram with a variety of quantum phase transitions. The odd-parity superconductivity is preserved in this extension, but inter-band superconductivity is now present in addition to the intra-band ones. The presence of two-bands in our model allows us to include hybridization, increasing the space of parameters. We have considered symmetric and anti-symmetric hybridizations. Both are permitted, depending on the parities we choose for the angular momenta of the two orbitals.

We have calculated the self-consistent solutions for the inter- and intra-band superconducting order parameters as functions of the chemical potential and the strength of the symmetric or anti-symmetric hybridization. The self-consistent calculation of the order parameters allow to obtain the $T = 0$ phase diagram of the system. When increasing anti-symmetric hybridization, both intra- and inter-band superconductivity emerge in the phase diagram, but they compete and exclude one another for different values of band-filling. On the other hand, when increasing the symmetric hybridization, both types of superconductivity are present and they coexist. An interesting result is that inter-band superconductivity has the highest value of order parameter, indicating that it has

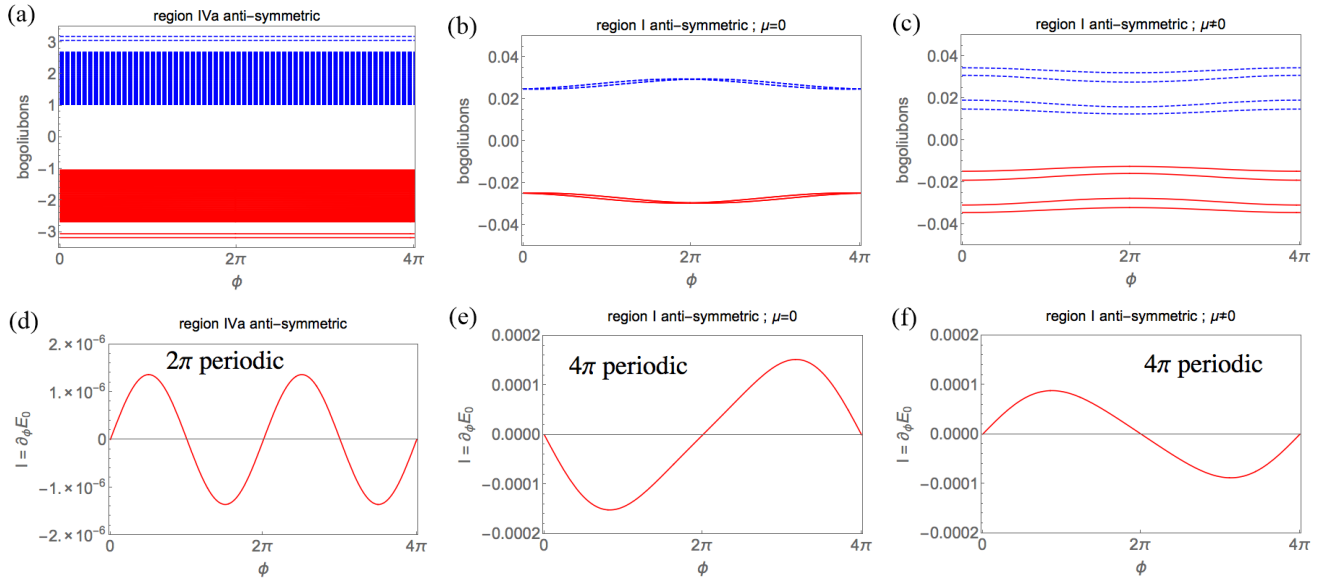


Figure 5. Results for anti-symmetric hybridization as we vary the tunneling phase ϕ : i) First row shows the excitation spectra that preserve the parity of the superconductor. ii) Second row shows the Josephson current flowing through the Josephson junction. Here we have used $L = 250$ and $t' = 0.1$.

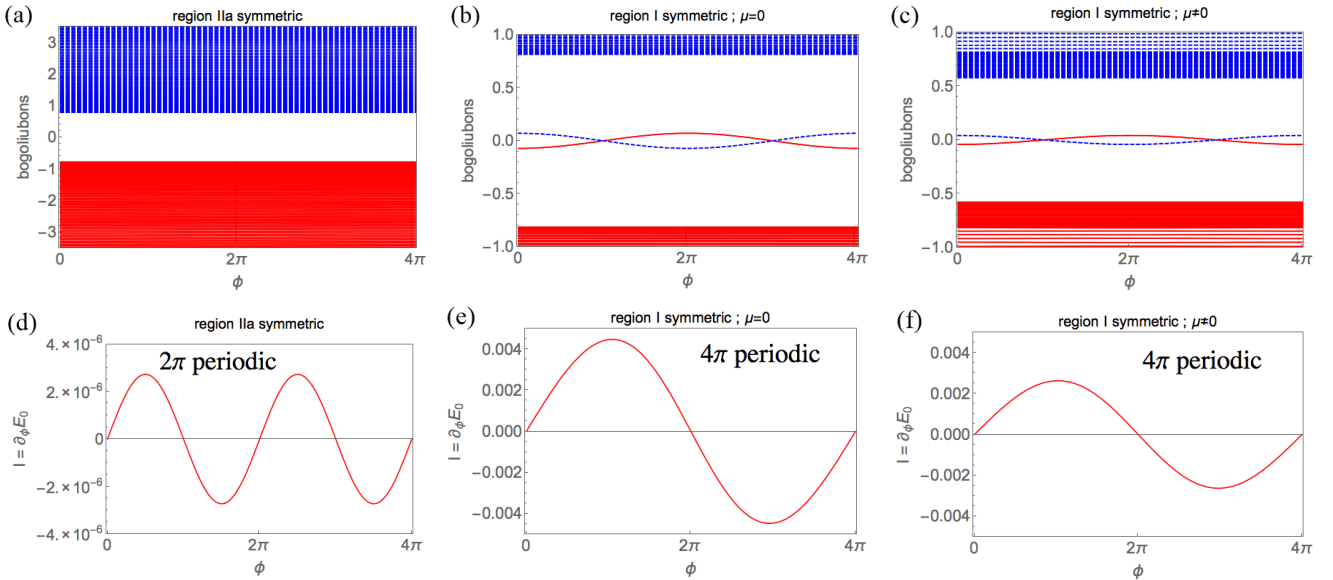


Figure 6. Results for the case of symmetric hybridization case as we vary the tunneling phase ϕ : i) First row shows the excitation spectrum that preserves the parity of the superconductor. ii) Second row shows the Josephson current through the Josephson junction. Here we have used $L = 150$ and $t' = 0.1$.

the higher critical temperature and makes it responsible for the superconductivity appearing in the system.

According to a general approach for obtaining the winding number of a system described by 4×4 matrices, a dominant inter-band coupling with symmetric hybridization between bands induces a topological superconducting phase. In order to further clarify our results concerning the nature of the topological phases and their end states, we have analyzed the energy spectrum of a

finite system.

In order to provide further evidence for the presence of edge Majorana states we have shown that in the topological phases one finds a 4π -periodic (fractional) Josephson current as one changes the magnetic flux across a ring composed of the superconductor with an insulator inserted between its ends. The result is consistent with the results for the winding number and edge states for the topological phase in the case of symmetric hybridiza-

tion. In addition, we also found the same 4π -periodic Josephson current in the hidden topological phase identified previously as Weyl-type in the case of anti-symmetric hybridization.

As a final note, we highlight that symmetric hybridization in addition to odd-parity inter-band superconductivity stabilizes a topological non-trivial phase, which presents localized states at the ends of the chain.

ACKNOWLEDGMENTS

The authors would like to thank the CNPq and FAPERJ for financial support. They also are grateful to Emilio Cobanera for discussion and calling attention to Ref. [75], and Griffith M.A.S. for useful discussions. Partial support from FCT through grant UID/CTM/04540/2013 is acknowledged.

REFERENCES

-
- * tharnier@me.com
- ¹ A. Y. Kitaev, *Physics-Uspekhi* **44**, 131 (2001).
 - ² A. Kitaev, *Annals of Physics* **303**, 2 (2003).
 - ³ J. Alicea, *Reports on Progress in Physics* **75**, 076501 (2012).
 - ⁴ M. Sato, Y. Takahashi, and S. Fujimoto, *Phys. Rev. Lett.* **103**, 020401 (2009).
 - ⁵ J. D. Sau, R. M. Lutchyn, S. Tewari, and S. Das Sarma, *Phys. Rev. Lett.* **104**, 040502 (2010).
 - ⁶ L. Fu and C. L. Kane, *Phys. Rev. Lett.* **100**, 096407 (2008).
 - ⁷ A. C. Potter and P. A. Lee, *Phys. Rev. B* **83**, 184520 (2011).
 - ⁸ E. Wang, H. Ding, A. V. Fedorov, W. Yao, Z. Li, Y.-F. Lv, K. Zhao, L.-G. Zhang, Z. Xu, J. Schneeloch, R. Zhong, S.-H. Ji, L. Wang, K. He, X. Ma, G. Gu, H. Yao, Q.-K. Xue, X. Chen, and S. Zhou, *Nat Phys* **9**, 621 (2013).
 - ⁹ V. Mourik, K. Zuo, S. M. Frolov, S. R. Plissard, E. P. A. M. Bakkers, and L. P. Kouwenhoven, *Science* **336**, 1003 (2012), <http://www.sciencemag.org/content/336/6084/1003.full.pdf>.
 - ¹⁰ S. Nadj-Perge, I. K. Drozdov, B. A. Bernevig, and A. Yazdani, *Phys. Rev. B* **88**, 020407 (2013).
 - ¹¹ S. Nadj-Perge, I. K. Drozdov, J. Li, H. Chen, S. Jeon, J. Seo, A. H. MacDonald, B. A. Bernevig, and A. Yazdani, *Science* **346**, 602 (2014), <http://www.sciencemag.org/content/346/6209/602.full.pdf>.
 - ¹² P. D. Sacramento, *Journal of Physics: Condensed Matter* **27**, 445702 (2015).
 - ¹³ F. Pientka, L. I. Glazman, and F. von Oppen, *Phys. Rev. B* **88**, 155420 (2013).
 - ¹⁴ P. M. R. Brydon, S. Das Sarma, H.-Y. Hui, and J. D. Sau, *Phys. Rev. B* **91**, 064505 (2015).
 - ¹⁵ H.-Y. Hui, P. M. R. Brydon, J. D. Sau, S. Tewari, and S. D. Sarma, *Scientific Reports* **5**, 8880 (2015).
 - ¹⁶ T. Watanabe, T. Yoshida, and Y. Yanase, *ArXiv:1508.01333 [cond-mat.supr-con]* (2015), [arXiv:1508.01333 \[cond-mat.supr-con\]](https://arxiv.org/abs/1508.01333).
 - ¹⁷ D. Vollhardt and P. Wolfe, *The superfluid phases of Helium 3* (Courier Corporation, 2013).
 - ¹⁸ A. P. Mackenzie and Y. Maeno, *Rev. Mod. Phys.* **75**, 657 (2003).
 - ¹⁹ M. Sato and S. Fujimoto, *Phys. Rev. B* **79**, 094504 (2009).
 - ²⁰ K. Sun, C.-K. Chiu, H.-H. Hung, and J. Wu, *Phys. Rev. B* **89**, 104519 (2014).
 - ²¹ J. Kortus, *Physica C: Superconductivity* **456**, 54 (2007), recent *Advances in MgB2 Research*.
 - ²² X. X. Xi, *Reports on Progress in Physics* **71**, 116501 (2008).
 - ²³ Y. Yang, W.-S. Wang, Y.-Y. Xiang, Z.-Z. Li, and Q.-H. Wang, *Phys. Rev. B* **88**, 094519 (2013).
 - ²⁴ S. Yin, J. E. Baarsma, M. O. J. Heikkinen, J.-P. Martikainen, and P. Törmä, *ArXiv:1508.05321 [cond-mat.quant-gas]* (2015), [arXiv:1508.05321 \[cond-mat.quant-gas\]](https://arxiv.org/abs/1508.05321).
 - ²⁵ R. Nourafkan, G. Kotliar, and A.-M. S. Tremblay, *ArXiv:1508.01789 [cond-mat.supr-con]* (2015), [arXiv:1508.01789 \[cond-mat.supr-con\]](https://arxiv.org/abs/1508.01789).
 - ²⁶ K. Sun, W. V. Liu, A. Hemmerich, and S. Das Sarma, *Nat Phys* **8**, 67 (2012).
 - ²⁷ B. Liu, X. Li, B. Wu, and W. V. Liu, *Nat Commun* **5** (2014).
 - ²⁸ Y. Tanaka, *Superconductor Science and Technology* **28**, 034002 (2015).
 - ²⁹ V. Stanev, *Superconductor Science and Technology* **28**, 014006 (2015).
 - ³⁰ G. Go, J.-H. Park, and J. H. Han, *Phys. Rev. B* **87**, 155112 (2013).
 - ³¹ S.-Y. Lee, J.-H. Park, G. Go, and J. H. Han, *ArXiv e-prints* (2013), [arXiv:1312.6469 \[cond-mat.str-el\]](https://arxiv.org/abs/1312.6469).
 - ³² Y. He, J. Moore, and C. M. Varma, *Phys. Rev. B* **85**, 155106 (2012).
 - ³³ L. Fu and E. Berg, *Phys. Rev. Lett.* **105**, 097001 (2010).
 - ³⁴ L. Fu, *Phys. Rev. B* **90**, 100509 (2014).
 - ³⁵ A. C. Silva, M. A. N. Araújo, and P. D. Sacramento, *EPL (Europhysics Letters)* **110**, 37008 (2015).
 - ³⁶ R.-L. Chu, G.-B. Liu, W. Yao, X. Xu, D. Xiao, and C. Zhang, *Phys. Rev. B* **89**, 155317 (2014).
 - ³⁷ G. Xu, J. Wang, B. Yan, and X.-L. Qi, *Phys. Rev. B* **90**, 100505 (2014).
 - ³⁸ L. Li, E. V. Castro, and P. D. Sacramento, *Phys. Rev. B* **94**, 195419 (2016).
 - ³⁹ W. P. Su, J. R. Schrieffer, and A. J. Heeger, *Phys. Rev. Lett.* **42**, 1698 (1979).
 - ⁴⁰ R. Wakatsuki, M. Ezawa, Y. Tanaka, and N. Nagaosa, *Phys. Rev. B* **90**, 014505 (2014).
 - ⁴¹ B. Braunecker, G. I. Japaridze, J. Klinovaja, and D. Loss, *Phys. Rev. B* **82**, 045127 (2010).
 - ⁴² T.-P. Choy, J. M. Edge, A. R. Akhmerov, and C. W. J. Beenakker, *Phys. Rev. B* **84**, 195442 (2011).
 - ⁴³ M. Kjaergaard, K. Wölms, and K. Flensberg, *Phys. Rev. B* **85**, 020503 (2012).

- ⁴⁴ J. Klinovaja, P. Stano, A. Yazdani, and D. Loss, *Phys. Rev. Lett.* **111**, 186805 (2013).
- ⁴⁵ M. M. Vazifeh and M. Franz, *Phys. Rev. Lett.* **111**, 206802 (2013).
- ⁴⁶ J. Klinovaja and D. Loss, *Phys. Rev. X* **3**, 011008 (2013).
- ⁴⁷ B. Braunecker and P. Simon, *Phys. Rev. Lett.* **111**, 147202 (2013).
- ⁴⁸ I. C. Fulga, A. Haim, A. R. Akhmerov, and Y. Oreg, *New Journal of Physics* **15**, 045020 (2013).
- ⁴⁹ Y. Niu, S. B. Chung, C.-H. Hsu, I. Mandal, S. Raghu, and S. Chakravarty, *Phys. Rev. B* **85**, 035110 (2012).
- ⁵⁰ W. DeGottardi, M. Thakurathi, S. Vishveshwara, and D. Sen, *Phys. Rev. B* **88**, 165111 (2013).
- ⁵¹ A. Russo and S. Chakravarty, *Phys. Rev. B* **88**, 184513 (2013).
- ⁵² Q.-J. Tong, J.-H. An, J. Gong, H.-G. Luo, and C. H. Oh, *Phys. Rev. B* **87**, 201109 (2013).
- ⁵³ T. Čadež and P. D. Sacramento, *Journal of Physics: Condensed Matter* **28**, 495703 (2016).
- ⁵⁴ F. Deus, M. A. Continentino, and H. Caldas, *Annals of Physics* **362**, 208 (2015).
- ⁵⁵ K. T. Law, P. A. Lee, and T. K. Ng, *Phys. Rev. Lett.* **103**, 237001 (2009).
- ⁵⁶ M. Wimmer, A. R. Akhmerov, J. P. Dahlhaus, and C. W. J. Beenakker, *New Journal of Physics* **13**, 053016 (2011).
- ⁵⁷ A. V. Burmistrova, I. A. Devyatov, A. A. Golubov, K. Yada, and Y. Tanaka, *Journal of the Physical Society of Japan* **82**, 034716 (2013), <http://dx.doi.org/10.7566/JPSJ.82.034716>.
- ⁵⁸ A. Das, Y. Ronen, Y. Most, Y. Oreg, M. Heiblum, and H. Shtrikman, *Nat Phys* **8**, 887 (2012).
- ⁵⁹ M. A. N. Araújo and P. D. Sacramento, *Phys. Rev. B* **79**, 174529 (2009).
- ⁶⁰ M. Sato and S. Fujimoto, *Journal of the Physical Society of Japan* **85**, 072001 (2016), <http://dx.doi.org/10.7566/JPSJ.85.072001>.
- ⁶¹ T. Ojanen and T. Kitagawa, *Phys. Rev. B* **87**, 014512 (2013).
- ⁶² P. D. Sacramento, M. A. N. Araújo, and E. V. Castro, *EPL* **105**, 37011 (2014).
- ⁶³ R. M. Lutchyn, J. D. Sau, and S. Das Sarma, *Phys. Rev. Lett.* **105**, 077001 (2010).
- ⁶⁴ C. Xu and L. Fu, *Phys. Rev. B* **81**, 134435 (2010).
- ⁶⁵ L. Jiang, D. Pekker, J. Alicea, G. Refael, Y. Oreg, and F. von Oppen, *Phys. Rev. Lett.* **107**, 236401 (2011).
- ⁶⁶ Kwon, H.-J., Sengupta, K., and Yakovenko, V. M., *Eur. Phys. J. B* **37**, 349 (2004).
- ⁶⁷ H.-J. Kwon, V. M. Yakovenko, and K. Sengupta, *Low Temperature Physics* **30**, 613 (2004).
- ⁶⁸ Y. Oreg, G. Refael, and F. von Oppen, *Phys. Rev. Lett.* **105**, 177002 (2010).
- ⁶⁹ M. Cheng and R. M. Lutchyn, *Phys. Rev. B* **86**, 134522 (2012).
- ⁷⁰ F. Domínguez, F. Hassler, and G. Platero, *Phys. Rev. B* **86**, 140503 (2012).
- ⁷¹ K. T. Law and P. A. Lee, *Phys. Rev. B* **84**, 081304 (2011).
- ⁷² M. Gibertini, F. Taddei, M. Polini, and R. Fazio, *Phys. Rev. B* **85**, 144525 (2012).
- ⁷³ C. W. J. Beenakker, D. I. Pikulin, T. Hyart, H. Schomerus, and J. P. Dahlhaus, *Phys. Rev. Lett.* **110**, 017003 (2013).
- ⁷⁴ E. J. H. Lee, X. Jiang, M. Houzet, R. Aguado, C. M. Lieber, and S. De Franceschi, *Nat Nano* **9**, 79 (2014).
- ⁷⁵ A. Alase, E. Cobanera, G. Ortiz, and L. Viola, *ArXiv e-prints* (2016), arXiv:1601.05486 [cond-mat.supr-con].
- ⁷⁶ Y. Nambu, *Phys. Rev.* **117**, 648 (1960).
- ⁷⁷ T. O. Puel, P. D. Sacramento, and M. A. Continentino, *Journal of Physics: Condensed Matter* **27**, 422002 (2015).
- ⁷⁸ A. P. Schnyder, S. Ryu, A. Furusaki, and A. W. W. Ludwig, *Phys. Rev. B* **78**, 195125 (2008).
- ⁷⁹ K. Yada, M. Sato, Y. Tanaka, and T. Yokoyama, *Phys. Rev. B* **83**, 064505 (2011).
- ⁸⁰ A. Ii, K. Yada, M. Sato, and Y. Tanaka, *Phys. Rev. B* **83**, 224524 (2011).
- ⁸¹ K. Jiménez-García, L. J. LeBlanc, R. A. Williams, M. C. Beeler, A. R. Perry, and I. B. Spielman, *Phys. Rev. Lett.* **108**, 225303 (2012).